VCSEL polarization modulation for pulse-per-second clock signal transfer in optical frequency distribution systems

G. M. Isoe*, A. W. R. Leitch and T. B. Gibbon

Centre for Broadband Communication, Nelson Mandela University, Port Elizabeth 6031, South Africa

(Received 21 March 2018; Revised 27 April 2018)

In this paper, a novel vertical cavity surface emitting laser (VCSEL) polarization modulation technique based on polarization switching due to thermal heating in a single transverse mode class 10 G VCSEL at 1 310 nm is demonstrated experimentally. The inherent orthogonal polarization switching of the VCSEL carrier with changing bias is exploited in the transmission of pulse-per-second (PPS) timing clock signal. Experimental results show that PPS pulse widths of 9.97 μs and 9.98 μs are measured for back-to-back analysis and over 3.21 km of G 652 urban fibre transmission, respectively. This work provides a novel alternative for adoption in optical frequency and time transfer applications.

Document code: A **Article ID:** 1673-1905(2018)05-0376-4

DOI https://doi.org/10.1007/s11801-018-8042-9

Optical time and frequency (TFR) transfer has recently become a major topic of research[1-3]. Among the technologies for time and frequency distribution, optical fibre based TFR links employing vertical cavity surface emitting laser (VCSEL) transmitters offer alternative solution in decreasing network cost, energy consumption and complexity. VCSELs have attracted much attention over years[4-6]. This is due to their promising applications in optical communication, optical signal processing and optical interconnect[7,8].

VCSEL polarization modulation is a relatively simple, low complexity alternative modulation approach. VCSELs usually emit linearly polarized light, oriented in a specific crystallographic direction[9]. This is mainly due to their cylindrical symmetry, direction of lasing, and carrier injection. The carrier injection is always perpendicular to the active layer and along the axis of cylindrical symmetry[10,11].

However, during VCSEL's manufacturing process, some inherent birefringence caused by stresses unintentionally induced my lead to polarization switching of the VCSEL device[9]. The linearly polarized light emitted from VCSEL lasers has therefore been reported to switch between two orthogonal states[12]. The output light of VCSELs can exist in two orthogonal modes along $\langle 011 \rangle$. The crystal mode directions are denoted as $P_{\parallel}$ and $P_{\perp}$, respectively. Current heating of the VCSEL active region changes the transverse refractive index profile by thermo-optic effect and leads to a creation of waveguide. As a result, the modal gain (G_{m}) for the fundamental Gaussian transverse mode is given as[13]

$$G_{\mathrm{m}} = g - \frac{\Delta g}{Sk_0}(2\eta_0 \Delta \eta)^{-(1/2)}, \tag{1}$$

where g is the gain in the center of the active region with a circular symmetry, Δg and $\Delta \eta$ are the gain and the refractive index differences between the center and the edge of the effective contact respectively, due to carrier spreading and effective contact[14]. S is the radius of the effective contact, η_0 is the effective refractive index, and $k_0=2\pi/\lambda_0$ where λ_0 is the wavelength in free space.

Considering that at resonance $\eta_0 L=N(\lambda_0/2)$, where L is the cavity length and N is an integer, Eq.(1) can be transformed into

$$G_{\mathrm{m}} = g\left\{1-\frac{1}{2\pi S}\sqrt{\frac{L}{N\dfrac{\mathrm{d}n}{\mathrm{d}T}}}\frac{\Delta g}{g}\sqrt{\frac{\lambda_0}{\Delta T}}\right\} =$$

$$g\left\{1-k\sqrt{\frac{\lambda_0}{\Delta T}}\right\} = g\left\{1-k\sqrt{\frac{\lambda_0}{A}}\frac{1}{\sqrt{P_{\mathrm{dis}}}}\right\}, \tag{2}$$

where $\Delta T=AP_{\mathrm{dis}}$, and P_{dis} is the power dissipated in VCSEL. The terms in parenthesis in Eq.(2) describe the effect of the thermal wave guiding which is more effective for smaller wavelengths and larger temperature difference ΔT.

Pulse-per-second (PPS) clock signals have attracted vast interests in timing applications such as coordinated universal time (UTC) and global positioning systems (GPS). This is mainly due to its low jitter, high accuracy and precision[15]. Fibre based communication networks also play an increasingly important role in dissemination of present and future time and frequency standards, for emerging optical frequency standards and clocks. Through intelligent network design and active correction mechanisms to compensate for fibre induced propagation mitigation and its resultant impact on reference clock instability, optical fibres are ideal alternative for optical frequency standards transfer[3,16-18].

* E-mail: George.Isoe@nmmu.ac.za

This work reports a novel VCSEL polarization modulation exploiting the VCSEL polarization switching mechanism due to thermal lensing. A PPS timing clock signal is modulated onto the polarization states of a single mode VCSEL carrier at 1 310 nm, by exploiting the inherent orthogonal polarization switching of a VCSEL carrier with changing bias. Our modulation approach requires polarization switching when injection levels into two superimposed polarization maintaining waveguides change magnitude. This also implies that the polarization maintaining waveguides must have strong polarization selectivity. With our proposed VCSEL polarization modulation technique, it is possible to achieve a higher extinction ratio between the two digital states (the 1's and 0's) without high peak-to-peak voltage (V_{pp}). This is due to the orthogonality of the polarization states (such as horizontal and vertical polarization).

Fig.1 shows the experimental setup used to demonstrate VCSEL polarization dynamics, by investigating the polarization-resolved light-current characteristics of the VCSEL carrier.

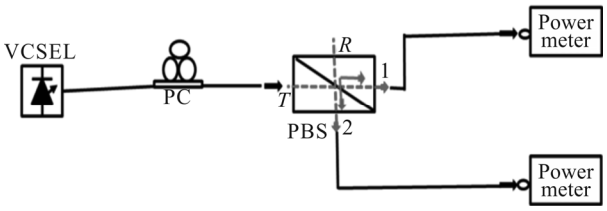

PC: polarization controller; PBS: polarization beam splitter

Fig.1 VCSEL polarization dynamic experimental setup

A single transverse-mode commercial class 10 G VCSEL designed for high-speed performance (10 GHz bandwidth) is considered for analysis. Polarization-independent parameters of a similar device have been reported in Ref.[19]. This laser has an emission wavelength of 1 307.05 nm at I=7.01 mA and a threshold current of 1.53 mA. As shown in Fig.1, the optical light output from the VCSEL under test was connected with the input port of a polarization beam splitter. The polarization beam splitter was used to separate the incoming VCSEL light into its respective orthogonal states. A polarization controller was used to align the states of polarization (SOP) orientation of the incoming VCSEL light wave to ensure that the SOP of the incoming light wave is a resultant of the two orthogonal states of polarization. This was enabled by monitoring the output power of the two optical power meters while turning the polarization controller up until the two power meters' reading was at the same level.

The light launched along the slow axis of input port T will be transmitted along the slow axis of output port 1 and measured using power meter 1 as shown in Fig.1. Consequently, the light launched along the fast axis of input port T will be transmitted along the slow axis of output port 2 and measured with power meter 2. Polarization maintaining fibres were used to connect output 1 and 2 with their respective power meters to maintain their SOPs. The VCSEL polarization-resolved light-current measurements were taken by varying the bias current from 1 mA to 9.97 mA while recording the respective output power of the two meters.

The experimentally measured VCSEL polarization resolved light currents are shown in Fig.2. A polarization switching from the high frequency (*Y*-mode) to the low frequency (*X*-mode) polarization mode was observed near 4.68 mA bias current. The *X*-mode and the *Y*-mode were orthogonal to each other. No appreciable hysteresis was observed. At this polarization switching point (4.68 mA), no drop of the total output power was observed.

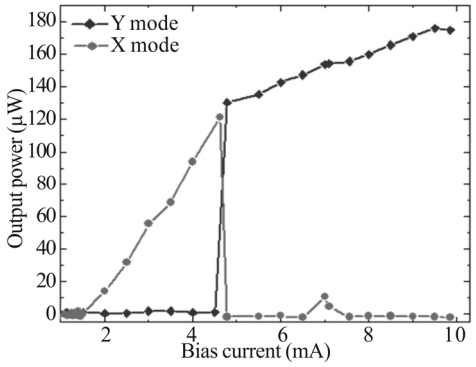

Fig.2 Polarization resolved light-current characteristics of a free running VCSEL

Results in Fig.2 prove a key polarization dynamic ability of VCSEL transmitters. From these polarization-resolved light-current measurements, VCSEL polarization switching between two orthogonal states of polarization was achieved at 4.68 mA bias current. In this experimental demonstration, the external temperature of the VCSEL was maintained at room temperature (about 25 °C) using a thermal electric cooler (TEC) circuit so that temperature effects could not come into play.

To further demonstrate VCSEL polarization switching between two orthogonal states of polarization for the realization of VCSEL polarization modulation, the VCSEL was biased at 4.68 mA as demonstrated in our previous contributions[6,20]. This biased point was carefully selected so that any slight increase or decrease in current could result in a switching in states of polarization of the VCSEL from polarization region “A” to polarization region “B” and vice-versa as shown in Fig.3. At a bias current of exactly 4.68 mA, the VCSEL was noted to be lasing at polarization state “A”. However, a 0.2 mA increase in bias current was noted for a polarization switching from polarization state “A” to polarization state “B” as shown in Fig.4, therefore achieving VCSEL polarization switching. A polarization analyzer was used to monitor the polarization characteristics of the VCSEL under test thus collecting polarization results used in Fig.4. This mechanism was therefore adopted to realize the VCSEL polarization modulation using a PPS clock signal as our previous contribution in Ref.[20]. A rubidium frequency standard model FS725 was adopted to generate 1 PPS electrical signal with pulse width of

10 μs used in this contribution. The electrical 1 PPS signal voltage was attenuated by 42 dBm.

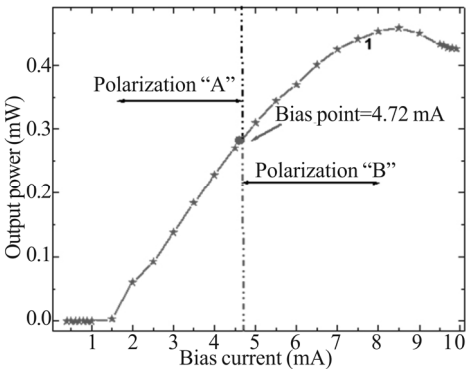

Fig.3 VCSEL bias characteristic curve

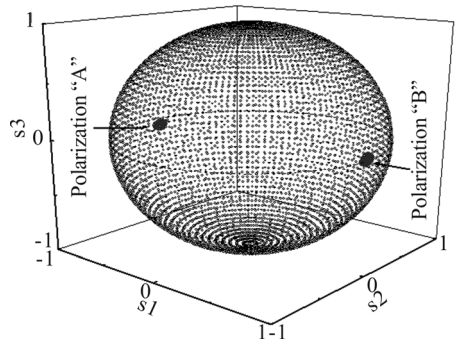

Fig.4 Poincaré sphere showing the two orthogonal polarization states of a VCSEL due to polarization switching after being modulated with a pulse per second signal

Due to the unavailability of a polarization-sensitive photodiode in our laboratory, it was important to develop a reliable technique that could recover the polarization-based PPS clock signal to intensity attribute, for its direct detection with an intensity-sensitive PIN photo receiver can be realized. To achieve this, a linear optical polarizer was used as shown in Fig.5.

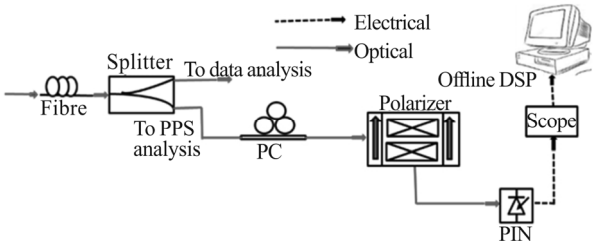

Fig.5 Experimental setup used to recover polarization-based PPS clock signal

Firstly, it is important to note that optical fibres are expected to maintain the same state of polarization of the input light wave throughout their transmission lengths. However, due to birefringence and mode coupling arising from different affecting conditions within the optical fibre link, the polarization stability of the optical light is altered. Polarization controllers were therefore used to realign polarization states of the VCSEL light wave to match with that of the linear polarizer. A 3.21 km transmission over ITU-T G.652 single mode urban fibre was experimentally achieved. This optical fibre has zero dispersion performance at 1 310 nm transmission window. The received PPS electrical signal was then captured using an Agilent sampling scope for offline statistical analysis.

The statistical PPS pulse width results of the received polarization based PPS clock signal after its transmission over 3.21 km of G.652 optical fibre are presented in Fig.6. These measurements were conducted by taking the time difference between the rising edge and falling edge of individual received PPS pulse signals at full width at half maximum (*FWHM*). PPS pulse widths of 9.97 μs and 9.98 μs were attained for back-to-back (B2B) and 3.21 km fibre transmission, respectively, corresponding to deviations of −0.03 μs and −0.02 μs respectively from the 1 PPS actual pulse width of 10.00 μs as stated in Ref.[21]. These deviations were contributed by the cumulative equipment error. It is noted that the PPS pulse peak presents slight distortion upon its detection. This is due to chirping property of the VCSEL laser source. However, this did not affect the integrity of the rising and falling edges of the PPS clock signal as seen in Fig.6. This is the key requirement for timing clock signals in time and frequency reference application systems.

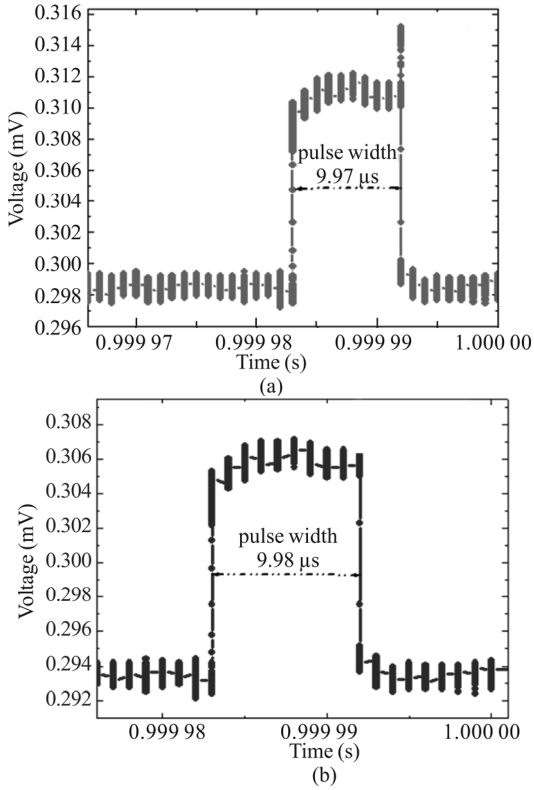

Fig.6 PPS measured pulse widths for (a) back-to-back and (b) 3.21 km of G.652 fibre transmission

A frequency count distribution of the measured time between successive pulses is presented in Fig.7. The results were obtained by taking the time difference between the rising edge of the first pulse and that of each successive pulse.

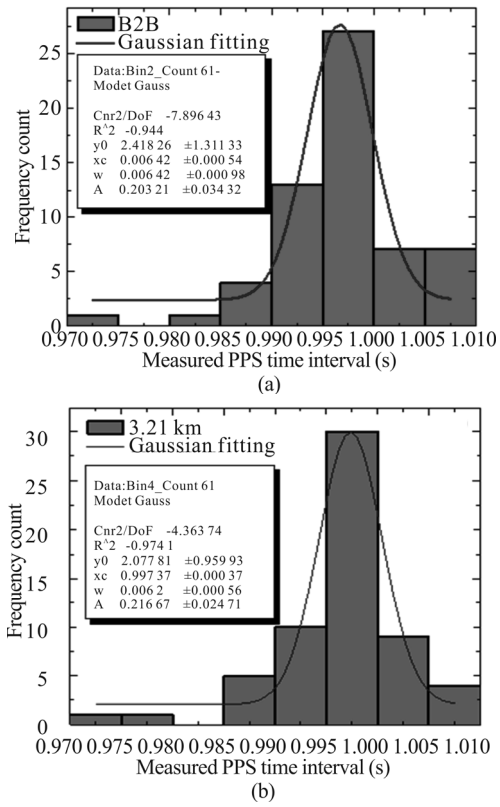

Fig.7 Time frequency count measurement for (a) back-to-back and (b) 3.21 km of G. 652 fibre transmission

In our analysis, 60 pulses were considered in total. From the results in Fig.6, a maximum count was seen at 1 s for all experimental scenarios considered. This implies that the PPS clock signal retained its timing property (a pulse every second) even after a fibre transmission.

Optical communication plays an extremely important role in both telecommunication networks and time and frequency reference systems. Clock and reference frequency signal distribution is of great importance in UTC, GPS, banks and big data science projects. We have shown the VCSEL polarization modulation based on VCSEL polarization switching mechanism due to thermal lensing. A PPS has been modulated successfully into the polarization states of a single mode VCSEL and a fibre transmission of 3.21 km was achieved. The 3.21 km SMF transmission length suits timing application in the optical access network. Our proposed VCSEL polarization modulation technique complies with strict power consumption, cost and size limitations, thus allows for integration within an already existing optical fibre network. The VCSEL polarization modulation technology is demonstrated using a PPS timing clock signal with pulse width of 10 μs due to its availability in our laboratory. However, higher reference clock frequencies can still be supported in the same network system where splitting ratio and reach capacity can be traded off against one another to enhance the system performance. In addition, innovative network design aiming at reducing the overall network cost and complexity through shared infrastructure is an ideal alternative to address connectivity issues in optical frequency distribution systems.

References

[1] Ł. Śliwczyński, P. Krehlik, A. Czubla, Ł. Buczek and M. Lipiński, Metrologia **50**, 133 (2013).

[2] S. Li, C. Wang, H. Lu and J. Zhao, IEEE Photonics Journal, 99 (2017).

[3] X. Chen, J. Lu, Y. Cui, J. Zhang, X. Lu and X. Tian, Scientific Reports **5**, 18343 (2015).

[4] D. M. Kuchta, High Capacity VCSEL-based Links, Optical Fiber Communications Conference and Exhibition (OFC), 1 (2017).

[5] S. Wassin, G. M. Isoe, R. R. G. Gamatham, A. W. R. Leitch and T. B. Gibbon, Optics & Laser Technology **105**, 66 (2018).

[6] G. Isoe, S. Wassin, R. Gamatham, A. Leitch and T. Gibbon, Journal of Modern Optics **64**, 2245 (2017).

[7] E. Haglund, Å. Haglund, J. S. Gustavsson, B. Kögel, P. Westbergh and A. Larsson, Reducing the Spectral Width of High Speed Oxide Confined VCSELs Using an Integrated Mode Filter, in Vertical-Cavity Surface-Emitting Lasers Xvi, 2012.

[8] N. Quadir, P. Ossieur and P. D. Townsend, A 56Gb/s PAM-4 VCSEL Driver Circuit, IET Irish Signals and Systems Conference (ISSC 2012), 1 (2012).

[9] A. J. Van Doorn, M. Van Exter and J. Woerdman, Applied Physics Letters **69**, 1041 (1996).

[10] A. Quirce, P. Pérez, A. Popp, A. Valle, L. Pesquera and Y. Hong, Semiconductor Lasers & Laser Dynamics VII, 98920Q (2016).

[11] P. Pérez, H. Lin, Á. Valle and L. Pesquera, Journal of the Optical Society of America B **31**, 2901 (2014).

[12] K. D. Choquette, D. Richie and R. Leibenguth, Applied Physics Letters **64**, 2062 (1994).

[13] H. Kawaguchi, I. Hidayat, Y. Takahashi and Y. Yamayoshi, Electronics Letters **31**, 109 (1995).

[14] N. Dutta, Journal of Applied Physics **68**, 1961 (1990).

[15] U. Schmid, M. Horauer and N. Kero, How to Distribute GPS-time over COTS-based LANs, DTIC Document, 545 (1999).

[16] Y. He, B. J. Orr, K. G. Baldwin, M. J. Wouters, A. N. Luiten and G. Aben, Optics Express **21**, 18754 (2013).

[17] M. T. Hsu, Y. He, D. A. Shaddock, R. B. Warrington and M. B. Gray, IEEE Photonics Technology Letters **24**, 1015 (2012).

[18] K. G. Baldwin, Y. He, M. Hsu, M. Wouters, M. Gray and B. J. Orr, Analog and All-digital Frequency Distribution via Optical Fiber Links, CLEO: Science and Innovations, CTh4A.2 (2012).

[19] P. Pérez, A. Valle, I. Noriega and L. Pesquera, Journal of Lightwave Technology **32**, 1601 (2014).

[20] G. M. Isoe, S. Wassin, R. R. G. Gamatham, A. W. R. Leitch and T. B. Gibbon, Simultaneous 10 Gbps Data and Polarization-based Pulse-per-second Clock Transmission Using a Single VCSEL for High-speed Optical Fibre Access Networks, Optical Metro Networks and Short-Haul Systems IX. International Society for Optics and Photonics, 101290F (2017).

[21] S. inc., FS725 Rubidium Frequency Standard Operation and Service Manual vol. Version 1.3. 1290-D Reamwood Avenue, Sunnyvale, California 94089: Stanford Research Systems, 2015.